ECOLOGY

Productivity-driven decoupling of microbial carbon use efficiency and respiration across global soils

Yongxing Cui[1,2]*, Shushi Peng[2], Manuel Delgado-Baquerizo[3], Daryl L. Moorhead[4], Robert L. Sinsabaugh[5], César Terrer[6], Thomas P. Smith[7], Yakov Kuzyakov[8,9], Josep Peñuelas[10,11], Biao Zhu[12], Feng Tao[13], Songbai Hong[14], Ji Chen[15]*, Matthias C. Rillig[1]

Despite extensive research on soil microbial carbon (C) use efficiency (CUE), its linkage to actual soil C storage remains ambiguous. A key uncertainty is that CUE estimates from short-term labeling incubations assume a linear negative relationship with respiration rates, overlooking nonlinear interactions and long-term microbial acclimation. Here, we use a stoichiometry-based approach to estimate CUE (CUE_{ST}), which links soil resource availability to microbial demand and captures microbial adaptability under resource constraints. We synthesized 1094 paired observations of CUE_{ST} and heterotrophic respiration rate (R_h) across natural ecosystems and found a nonlinear relationship between them governed by ecosystem productivity. In low-productivity arid and cold regions, CUE_{ST} declined with increasing R_h, whereas in productive tropical and temperate regions, CUE_{ST} stabilized at a low level (0.27 ± 0.11) as R_h exceeded 340 ± 10.8 grams of C per square meter per year. This shift reflects microbial trade-offs between C assimilation and stoichiometric homeostasis, revealing a decoupling of microbial growth from respiration that limits the capacity of productive ecosystems to store additional soil C.

INTRODUCTION

Soil microbial carbon (C) assimilation and heterotrophic respiration (R_h) are two basic microbial metabolic processes that collectively control organic C retention in soils (*1*–*3*). When the total microbial C uptake remains constant, higher assimilation for growth combined with lower R_h indicates more efficient biomass production, which enhances soil organic C retention (*4*–*6*). Culture-based studies, from strains to community levels, have shown that microbial growth efficiency is more stable than R_h under changing environmental conditions (*7*, *8*). Recent global assessments further suggest that warming accelerates R_h but does not have a clear or consistent effect on microbial growth (*9*, *10*).

These differential responses imply a decoupling between microbial C assimilation efficiency, commonly described as microbial C use efficiency (CUE), and R_h under specific environmental constraints. This decoupling challenges the long-held assumption that CUE uniformly declines with increasing R_h, even though CUE definitions vary among measurement approaches (*2*). It may also represent a key source of uncertainty in linking CUE to soil C storage and dynamics (*6*, *11*, *12*). Under nutrient-limited conditions, particularly low nitrogen (N) and phosphorus (P) availability, microorganisms may sustain growth by investing in energetically expensive enzyme production and efficient nutrient recycling, which increases C efflux while maintaining biomass production, thereby decoupling CUE from R_h (*13*, *14*). Nevertheless, this potential decoupling has been neither empirically tested across natural ecosystems nor understood in terms of the potential mechanisms involved.

This knowledge gap is likely attributable to three main reasons. First, most existing studies assume a linear negative relationship between CUE and R_h because widely used approaches, such as those based on $^{13}C/^{14}C$-labeled substrates and ^{18}O-labeled water, calculate CUE from pulse R_h and thus inherently generate a negative correlation between the two (*15*–*17*). However, this approach overlooks mounting evidence for widespread nonlinear relationships in soil C cycling across ecosystems (*7*, *18*). Second, R_h measurements used for estimating CUE are generally conducted on disturbed soils under short-term laboratory incubations, which reflect immediate metabolic responses to added substrates, rather than long-term microbial adaptability (*3*, *17*, *19*). Moreover, changes in the availability of one resource (e.g., C) can trigger cascading metabolic responses to other resources through priming effects and nutrient mining (*20*–*22*). These processes could obscure trade-offs between microbial C assimilation and the maintenance of stoichiometric homeostasis in natural ecosystems (*23*). Third, there is a lack of simultaneous, independent measurements of CUE and R_h across a range of natural ecosystems, limiting our ability to assess their relationship across environmental gradients.

To explore the potential decoupling between CUE and R_h, we compiled a global dataset of 1094 paired, independently derived observations of CUE and R_h across natural ecosystems. Specifically, we estimated CUE using a culture-independent stoichiometric model (*24*), which accounts for microbial enzyme allocation strategies to

[1]Institute of Biology, Freie Universität Berlin, Berlin 14195, Germany. [2]Sino-French Institute for Earth System Science, College of Urban and Environmental Sciences, Peking University, Beijing 100871, China. [3]Laboratorio de Biodiversidad y Funcionamiento Ecosistémico, Instituto de Recursos Naturales y Agrobiología de Sevilla (IRNAS), CSIC, Av. Reina Mercedes 10, E-41012 Sevilla, Spain. [4]Department of Environmental Sciences, University of Toledo, Toledo, OH 43606, USA. [5]Department of Biology, University of New Mexico, Albuquerque, NM 87131, USA. [6]Department of Civil and Environmental Engineering, Massachusetts Institute of Technology, Boston, MA 02139, USA. [7]Department of Life Sciences, Imperial College London, Silwood Park Campus, Ascot, Berkshire SL5 7PY, UK. [8]Department of Agricultural Soil Science, Department of Soil Science of Temperate Ecosystems, University of Goettingen, Goettingen 37077, Germany. [9]Peoples Friendship University of Russia RUDN University, Moscow 117198, Russia. [10]Global Ecology Unit CREAF-CSIC-UAB, CSIC, Bellaterra, Catalonia 08913, Spain. [11]CREAF, Cerdanyola del Vallès, Catalonia 08913, Spain. [12]State Key Laboratory for Vegetation Structure, Function and Construction (VegLab), Ministry of Education Key Laboratory for Earth Surface Processes, and College of Urban and Environmental Sciences, Peking University, Beijing, China. [13]Department of Ecology & Evolutionary Biology, Cornell University, Ithaca, NY 14853, USA. [14]School of Urban Planning and Design, Shenzhen Graduate School, Peking University, Shenzhen 518055, China. [15]State Key Laboratory of Loess Science, Institute of Earth Environment, Chinese Academy of Sciences, Xi'an 710061, China.
*Corresponding author. Email: cuiyongxing@zedat.fu-berlin.de (Y.C.); chenji@ieecas.cn (J.C.)

minimize elemental imbalances between soil resource supply and microbial growth demand. The estimated CUE ("CUE_{ST}" hereafter) reflects in situ microbial traits, with higher values indicating more efficient C utilization relative to nutrient acquisition. To obtain corresponding R_h values, we matched the geographic coordinates (latitude and longitude) of each CUE_{ST} observation with average annual R_h ("R_h" hereafter) from the latest global Soil Respiration Database (*25*), which characterizes long-term patterns of microbial respiration. We hypothesize that CUE_{ST} is negatively correlated with R_h under low C availability (e.g., low plant-derived C inputs), as microorganisms encounter a trade-off between C assimilation and respiratory loss. However, CUE_{ST} and R_h could decouple under low nutrient conditions because of increased C expenditure to acquire and recycle limiting nutrients, particularly N and P, to maintain stoichiometric homeostasis (Fig. 1). To test this hypothesis, we examined the relationship between CUE_{ST} and R_h across global ecosystems (Fig. 2A) and evaluated the environmental drivers with nine variables representing temperature, water, C, and nutrient availability.

RESULTS

Relationships between CUE and R_h at a global scale

We found that the relationship between CUE_{ST} and R_h varied across climatic zones and productivity levels. In arid and cold zones, CUE_{ST} declined significantly with increasing R_h ($P < 0.001$; Fig. 2B), whereas in tropical and temperate zones, it remained stable at a relatively low level (0.27 ± 0.11; $P > 0.05$). Because the shift in CUE_{ST}-R_h relationships across climate zones appeared to be strongly linked to ecosystem productivity, we categorized sites into low-productivity [leaf area index (LAI) < 3] and high-productivity (LAI > 3) ecosystems on the basis of the observed LAI range of 0.06 to 5.69 across sites. In low-productivity ecosystems, CUE_{ST} was negatively correlated with R_h ($n = 612$, $R^2 = 0.29$, $P < 0.001$; Fig. 2C), whereas this relationship was absent in high-productivity ecosystems ($n = 482$, $R^2 < 0.01$, $P = 0.20$). We further identified a global threshold of R_h at 340 ± 10.8 g C m^{-2} $year^{-1}$ (Fig. 3D and table S5). Below this threshold, CUE_{ST} declined significantly with increasing R_h ($n = 361$, $R^2 = 0.23$, $P < 0.001$); above it, no significant correlation was detected ($n = 733$, $R^2 < 0.01$, $P = 0.53$).

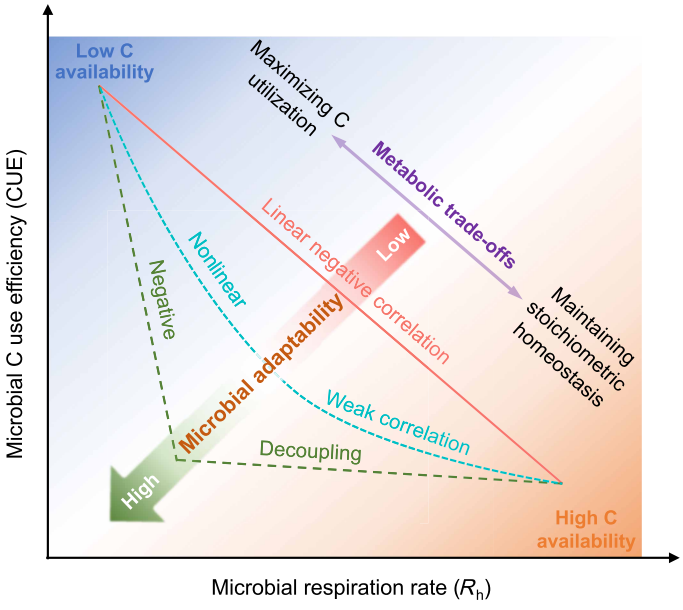

Fig. 1. Conceptual framework illustrating the possible relationships between microbial CUE and R_h on the basis of stoichiometric theory and microbial community theory. The stoichiometric theory suggests a linear negative relationship between CUE and R_h, as microorganisms respire excess C, e.g., via overflow respiration to maintain their elemental stoichiometric homeostasis, thereby reducing CUE as R_h increases (*4*, *69*). However, the relationship between CUE and R_h may become nonlinear or even decoupled (i.e., no correlation) with increasing resource availability and microbial physiological adaptation. Microbial adaptation tends to stabilize CUE, whereas increasing resource availability, particularly C, can disproportionately elevate R_h (*33*, *70*–*72*). Note that the specific meaning of CUE depends on the approaches used for its determination; here, it generally refers to the C assimilation efficiency of the microbial community.

Further support for decoupling between CUE and R_h was provided by two additional independent datasets: average daily R_h ($n = 52$) and $^{13}C/^{18}O$-measured CUE ($n = 132$) (Fig. 3 and fig. S7). First, CUE_{ST} was uncorrelated with average daily R_h in tropical and temperate zones ($P > 0.05$; Fig. 3A) but decreased significantly with average daily R_h in the cold zone ($R^2 = 0.80$, $P < 0.001$). Along a productivity gradient, a negative relationship was observed in low-productivity ecosystems ($R^2 = 0.28$, $P = 0.001$; Fig. 3B), whereas no significant correlation was found in high-productivity ones ($P = 0.08$). Across all sites, we identified a threshold of average daily R_h at 6.0 ± 1.4 g C m^{-2} day^{-1} (Fig. 3C and table S7): Below this threshold, CUE_{ST} declined significantly with average daily R_h ($R^2 = 0.28$, $P < 0.001$); above it, the relationship was not significant ($P = 0.76$). Note that this daily R_h threshold (equivalent to ~2190 g C m^{-2} $year^{-1}$ when multiplied by 365 days) is about 6.4 times higher than the annual R_h threshold described above (340 g C m^{-2} $year^{-1}$). This discrepancy is expected given that daily rates are usually measured during the growing season, whereas average annual values integrate fluxes across the entire year. Second, using the $^{13}C/^{18}O$-CUE dataset, we found a weak but significant negative correlation of $^{13}C/^{18}O$-CUE with R_h across all sites ($P = 0.02$; Fig. 3D). Regionally, $^{13}C/^{18}O$-CUE declined with R_h in the temperate zone ($R^2 = 0.21$, $P < 0.001$; Fig. 3E) but was decoupled in the cold zone ($P = 0.98$). A negative relationship was also observed in low-productivity ecosystems ($R^2 = 0.22$, $P < 0.001$; Fig. 3F), whereas no significant relationship was found in high-productivity ecosystems ($P = 0.77$).

Environmental drivers of the relationships between CUE and R_h

We used nine variables that represent the four fundamental controls (i.e., temperature, water, C, and nutrients) for microbial metabolism to further explore the environmental drivers underlying the relationship between CUE and R_h (Fig. 4). We expressed this relationship as the ratio of CUE_{ST} to R_h (hereafter "CUE_{ST}/R_h"), which reflects their relative changes across environmental gradients. A mixed-effects model selection analysis identified that these nine variables explain 68% of the variation in CUE_{ST}/R_h in low-productivity ecosystems, with seven of the nine variables, spanning all four basic controls, exerting significant effects ($P < 0.001$; Fig. 4A). In contrast, the nine variables explained only 32% of the variation in high-productivity ecosystems, with only three (related to temperature and nutrients) showing significant effects ($P < 0.001$; Fig. 4B). Generalized linear models further confirmed that nearly all nine variables had stronger effects (i.e., higher R^2 values) on CUE_{ST}/R_h in low-productivity ecosystems compared to high-productivity ones

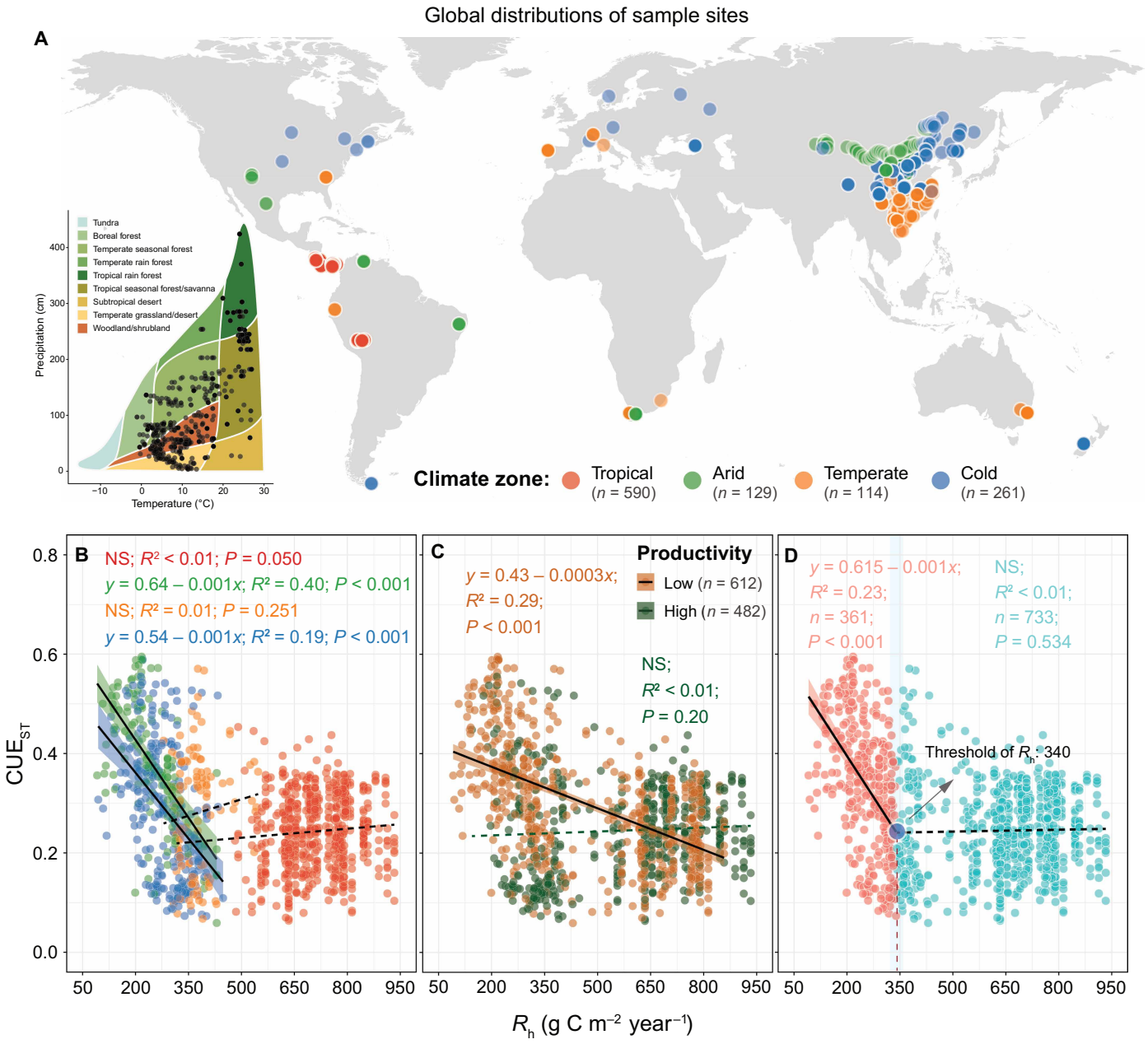

Fig. 2. Geographic distributions of sample sites and relationships between CUE_{ST} and average annual R_h. (**A**) A total of 1094 observations at 447 sites from 160 studies were collected for estimating CUE_{ST} using a stoichiometric-based method and are distributed across nearly all Whittaker biomes and major climatic zones. (**B** and **C**) Relationships between CUE_{ST} and R_h among climate zones (B) as well as in low-productivity (LAI < 3) and high-productivity (LAI > 3) ecosystems (C) were identified using generalized linear models. The shaded area is the 97.5% confidence interval of the linear regressions. All continuous lines are significant at $P < 0.05$, whereas dashed lines are not significant (NS; $P > 0.05$). (**D**) CUE_{ST} decoupled from R_h when $R_h > 340 \pm 10.8$ g C m^{-2} $year^{-1}$. The threshold of R_h was estimated using piecewise regression analyses (see table S5 for detailed results), and the relationships between CUE_{ST} and R_h before and after this threshold were identified using generalized linear models. The blue circle indicates the threshold of R_h, and the shaded area is the 97.5% confidence interval of the threshold. The solid black lines indicate model fits between CUE_{ST} and R_h ($P < 0.05$).

(Fig. 4C). These results suggest that in low-productivity ecosystems, CUE_{ST}-R_h relationships are shaped by a broad suite of environmental factors, whereas in high-productivity ecosystems, they are primarily governed by temperature and nutrient availability.

To better understand these patterns across climate zones, we focused on four key indicators [i.e., mean annual soil temperature (soil MAT), mean annual precipitation (MAP), LAI, and soil pH], each representing one of the four basic controls. These factors varied significantly across climatic zones ($P < 0.001$; fig. S11). Among them, soil pH exerted the strongest influence on CUE_{ST}/R_h in tropical and temperate zones, while MAP and LAI were the most influential in arid and cold zones, respectively (fig. S12). Furthermore, multiple

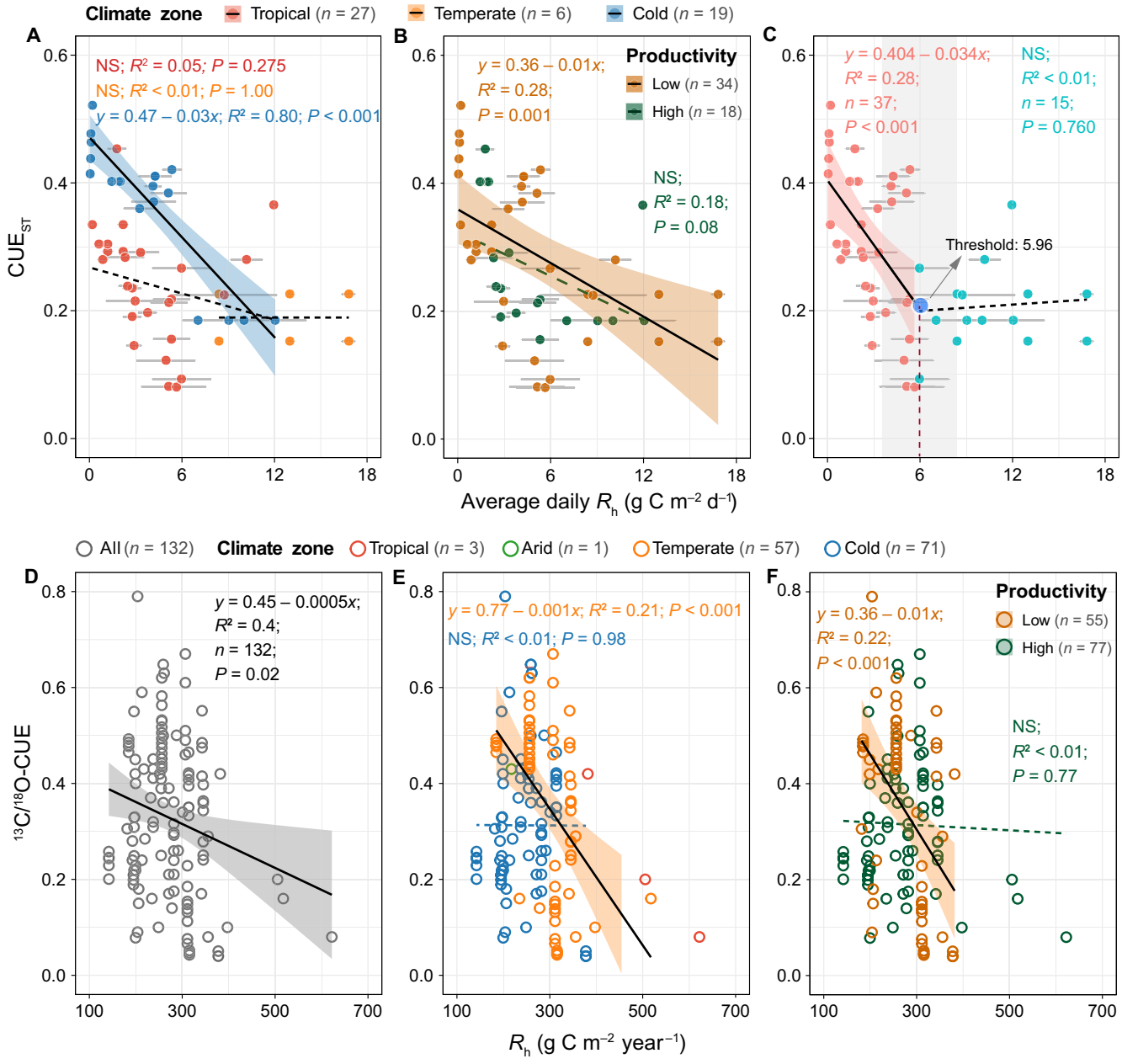

Fig. 3. Relationships between CUE_{ST} and average daily R_h or between $^{13}C/^{18}O$-CUE and average annual R_h across global soils. (**A** and **B**) Relationships between CUE_{ST} and average daily R_h among climatic zones (or in low- and high-productivity ecosystems) were identified using generalized linear models. The shaded area is the 97.5% confidence interval of the linear regressions. All continuous lines are significant at $P < 0.05$, whereas dashed lines are not significant ($P > 0.05$). (**C**) CUE_{ST} decoupled with average daily R_h when the average daily R_h was larger than the threshold of 5.96 ± 1.44 g C m^{-2} day^{-1}. The threshold of average daily R_h was estimated using piecewise regression analyses (see table S6 for detailed results), and the relationships between CUE_{ST} and average daily R_h before and after this threshold of average daily R_h were identified using generalized linear models. The blue circle indicates the threshold of average daily R_h, and the shaded area is the 97.5% confidence interval of the threshold. The solid black lines indicate model fits between CUE_{ST} and average daily R_h ($P < 0.05$). In (A) to (C), the gray line through each data point represents the standard deviation of the mean of average daily R_h. (**D** to **F**) Relationships between $^{13}C/^{18}O$-CUE and R_h among climatic zones (or in low- and high-productivity ecosystems) were identified using generalized linear models. Note that (i) no matching data of CUE_{ST} with average daily R_h were collected in the arid zone; (ii) we also did not fit the relationships between $^{13}C/^{18}O$-CUE and R_h for the tropical and arid zones in (E) because of the small number of observations, (iii) no threshold of R_h was identified in the relationship between $^{13}C/^{18}O$-CUE and R_h using piecewise regression analyses.

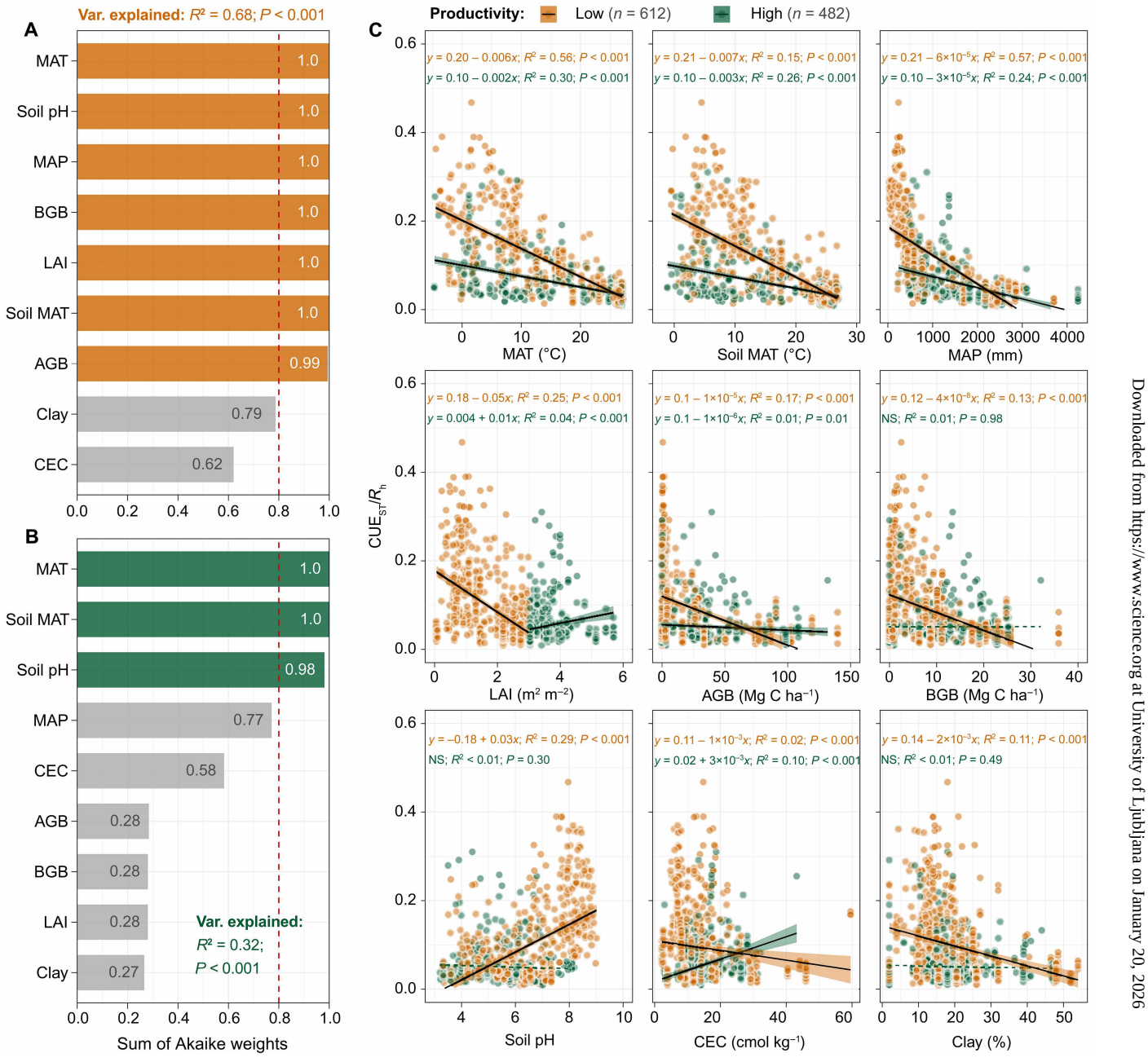

Fig. 4. Effects of environmental factors on the relative change of CUE_{ST} versus average annual R_h in low- and high-productivity ecosystems. (**A** and **B**) The analysis of mixed-effects model selection was used to evaluate the relative importance of these variables affecting CUE_{ST}/R_h. Values of the sum of Akaike weights were estimated on the basis of corrected Akaike's information criteria. A threshold value of 0.8 (red dashed line) was set to identify the most important variables. (**C**) The effects of these environmental variables on CUE_{ST}/R_h in low- and high-productivity ecosystems were also evaluated using generalized linear models. The shaded area is the 97.5% confidence interval of the linear regressions. All continuous lines are significant at $P < 0.05$, whereas dashed lines are not significant ($P > 0.05$). The relative change of CUE_{ST} versus R_h is expressed by the CUE_{ST}:R_h ratio (CUE_{ST}/R_h). Clay, soil clay content.

statistical analyses consistently showed that LAI, soil MAT, and MAP were the lowest in arid and cold zones, where they had strong negative effects on CUE_{ST} but strong positive effects on R_h (figs. S13 to S15). These contrasting influences likely contributed to the negative CUE_{ST}-R_h relationships observed in these zones (fig. S16). In contrast, in tropical and temperate zones, soil pH had the greatest positive effect on CUE_{ST}, while soil MAT and MAP continued to enhance R_h (figs. S13 to S15). This divergence in environmental drivers likely underpins the decoupling of CUE_{ST} and R_h in tropical and temperate regions (fig. S16).

DISCUSSION

As expected from traditional viewpoints, we found a negative relationship between CUE and R_h, a pattern that primarily occurred in low-productivity arid and cold regions (Fig. 2). This pattern likely

arises from a microbial trade-off between C assimilation and respiratory loss under limited plant-derived C inputs. In an environment with limited bioavailable C, microorganisms prioritize C allocation to anabolic processes over respiration (*20*, *26*), resulting in higher CUE relative to R_h. In addition, low temperatures and/or limited water availability in less productive ecosystems (fig. S11) suppress microbial metabolic rates, leading to a low R_h (*27*). These environmental constraints on water, temperature, and C tightly couple CUE with R_h in low-productivity ecosystems, likely contributing to the observed negative relationship.

Conversely, in high-productivity ecosystems, the decoupling between CUE and R_h (Fig. 3) supported our hypothesis that CUE does not continuously decline with increasing R_h under relatively high C inputs with low nutrient availability (i.e., generally high C:N:P ratios in substrates) (Fig. 1). High-productivity ecosystems, particularly in tropical regions, often experience strong P limitation (*28*–*30*) because of intense weathering, nutrient leaching, and high biotic demand (*31*, *32*). Despite these limitations, microbial communities appear capable of maintaining stoichiometric homeostasis for survival and growth. Long-term environmental filtering and adaptation may allow microorganisms to physiologically acclimate to nutrient scarcity (*33*–*35*). Two key mechanisms likely underpin the observed stability of CUE in high-production environments. First, microorganisms invest C and energy producing extracellular enzymes to acquire limiting nutrients (*24*), a process especially prevalent in tropical soils with high phosphatase activity (*29*, *36*, *37*). Second, microorganisms can exhibit high efficiency in recycling nutrients relative to C (*14*), preserving nutrients for growth while incurring losses of C and energy. These mechanisms help stabilize CUE at a relatively low level, even as R_h increases under sufficient temperature, water, and C conditions.

This shift in the CUE-R_h relationship along a productivity gradient carries important implications for soil C retention. In low-productivity ecosystems, high CUE coupled with low R_h (Fig. 2) suggests a strategy of maximizing C assimilation under limited C inputs, thereby enhancing microbial retention of plant-derived C despite low primary productivity. This finding aligns with decomposition model simulations indicating greater plant-to-soil C transfer efficiency in less productive ecosystems (*38*). In contrast, in high-productivity ecosystems, the decoupling of CUE from R_h (Fig. 2) implies that microorganisms invest excess C to acquire limiting nutrients, consistent with the frameworks of microbial stoichiometric homeostasis and nutrient mineralization (*39*, *40*). This strategy lowers the retention efficiency of plant-derived C in microbial biomass, leading to higher CO_2 release through R_h given high C inputs coupled with limiting nutrient availability.

Our results also suggest divergent trajectories of microbial C retention under various environmental changes. In low-productivity ecosystems (e.g., arid and cold regions), increased primary productivity due to CO_2 fertilization, warming, or enhanced precipitation (*41*–*43*) could disrupt the current CUE-R_h coupling. Increased plant C inputs may simultaneously raise R_h and reduce CUE, amplifying soil C efflux. Thus, vegetation greening in these regions (*41*, *44*) could paradoxically accelerate soil C losses. In contrast, high-productivity ecosystems (e.g., tropical and temperate regions) may show more stable soil C retention because of decoupling between CUE and R_h, regardless of changes in productivity. However, exogenous nutrient inputs such as atmospheric N and P deposition may alter this pattern. The historically low and stable CUE in high-productivity ecosystems could increase if nutrient limitations are alleviated, independent of changes in R_h (*45*, *46*). Rising atmospheric N and P deposition is enhancing soil nutrient availability, particularly in low-latitude regions (*47*, *48*), potentially boosting soil C sequestration in tropical and temperate ecosystems.

While our findings advance the understanding of microbial controls on soil C cycling, several uncertainties remain. First, we used R_h observations on the basis of geographic coordinates corresponding to our estimated CUE_{ST} to explore their relationships without accounting for fine-scale spatial and temporal mismatches. Such mismatches could obscure the relationships between microbial C use and respiration, although our sensitivity test still supports the results (figs. S2 and S3). We also acknowledge a potential mismatch in units between the parameters of CUE_{ST} (mass-based) and R_h (area-based), which could affect the relationship between CUE_{ST} and R_h. However, when R_h was converted from g C m^{-2} $year^{-1}$ to g C kg^{-1} $year^{-1}$ using soil bulk density, the observed patterns remained consistent (figs. S5 and S6 and table S5). Second, the uneven distribution of paired observations in our study may have also biased the relationships between CUE_{ST} and R_h. CUE_{ST} observations were mainly from China, Europe, and the Americas, with fewer observations from Africa and Russia (Fig. 2A). Further expanding the dataset would therefore be valuable for enhancing the robustness and applicability of the findings. Third, the use of soil pH, cation-exchange capacity (CEC), and clay content as proxies for nutrient availability introduces uncertainty. For example, soil pH differentially influences N and P availability (*49*) and can also affect microbial physiology (*50*–*52*). Last, although N and P are expected to be primarily limiting in temperate and tropical ecosystems, respectively (*28*–*30*), our analysis did not distinguish between their roles. Future research should aim at simultaneously and independently measuring microbial growth and R_h across temporal and spatial gradients, incorporating direct measures of particular nutrient status. Manipulative isotope-based experiments may also help clarify the trade-off between microbial C assimilation and efflux under resource constraints.

In summary, our study reveals unexpected and contrasting relationships between CUE and R_h across productivity gradients, supported by multiple lines of evidence, including independent datasets of average daily R_h and $^{13}C/^{18}O$-derived CUE. In low-productivity ecosystems, the coupling between CUE and R_h reflects a microbial strategy of prioritizing C assimilation. In contrast, the decoupling observed in high-productivity ecosystems indicates a shift toward nutrient acquisition and the maintenance of stoichiometric homeostasis. These findings imply a limited potential for natural ecosystems to serve as effective soil C sinks under global change (e.g., vegetation greening) and underscore the importance of incorporating microbial metabolic adaptability into future mechanistic assessments of soil C dynamics.

METHODS

Data collection

Global data of model parameters for estimating CUE_{ST}

We compiled a global database of ecoenzymatic activities, microbial biomass, and soil nutrient concentrations in surface soils (mean depth of 11 cm) from a survey of the literature using the Web of Science (http://isiknowledge.com) and the Google Scholar Resource Integrated Database (https://scholar.google.com). Combinations of keywords including "extracellular enzyme," "exoenzyme," "ecoenzyme,"

"threshold element ratio," "microbial C use efficiency," and "enzyme stoichiometry models" were used to search studies published from 1980 to 2022. The criteria for inclusion were as follows: (i) The studies included the activities of C-, N-, and P-acquiring enzymes [β-1, 4-glucosidase (BG), β-1, 4-*N*-acetylglucosaminidase (NAG), L-leucine aminopeptidase (LAP), and acid or alkaline phosphatase (AP)] (table S1); the concentrations of microbial biomass C, N, and P; and the concentrations of soil C [soil organic C (SOC)], N [total N (TN)], and P [total P (TP)], because these indicators are necessary parameters in the stoichiometric model of CUE_{ST} (*24*); (ii) the activities of extracellular enzymes were measured fluorometrically using a 200 μM solution of substrates labeled with 4-methylumbelliferone or 7-amino-4-methylcoumarin; (iii) microbial biomass was determined using chloroform fumigation-extraction; and (iv) data from intensively managed ecosystems (e.g., agroforests, fertilized plantations, sown pastures, croplands, and urban forests) were excluded to avoid influences from anthropogenic disturbances.

On the basis of these criteria, we selected 1094 paired observations across global terrestrial soils at 477 geographic locations from 160 articles (Fig. 2A). The data were extracted from tables or figures of the selected studies using GetData Graph Digitizer software version 2.25. We also recorded corresponding information on site location (longitude and latitude) from the literature. A PRISMA (Preferred Reporting Items for Systematic Reviews and Meta-Analyses) flow diagram (fig. S1) shows the procedure we used for selecting the studies. The dataset was also used by Cui *et al.* (*53*); the present study extends it by pairing each CUE_{ST} with R_h and conducts new analyses.

Global dataset of R_h

We extracted R_h values from the Soil Respiration Database (version 5.0; https://daac.ornl.gov/cgi-bin/dsviewer.pl?ds_id=1827) contributed by Jian *et al.* (*25*). A total of 1094 predictions of R_h were exactly matched to the sampling site coordinates of CUE_{ST} via raster data of R_h. In spite of exact matches in spatial coordinates of sampling sites between CUE_{ST} and R_h, we did not consider the differences in sampling time. However, given that all the sampling sites were from natural ecosystems without anthropogenic nutrient inputs or other major disturbance, the CUE_{ST} and R_h represent long-term adaptions of microbial communities to the environments in specific ecosystems. These facts should substantially reduce uncertainties in our results caused by mismatches in sampling or measurement times. We also considered that differences in the units of R_h may alter the relationship between CUE_{ST} and R_h, so we converted the units from g C m^{-2} $year^{-1}$ to g C kg^{-1} $year^{-1}$ via soil bulk density

$$R_h\left(\text{g C kg}^{-1}\ \text{year}^{-1}\right) = R_h\left(\text{g C m}^{-2}\ \text{year}^{-1}\right)/(\text{BD} \times h)$$

where BD is the soil bulk density (table S10; g cm^{-3}), and h is the soil depth (m). We defaulted h to 0.1 m because the mean soil depth was 0.114 m for the 1094 observations (*53*).

We found that values of mass-based R_h (g C kg^{-1} $year^{-1}$) were highly correlated with values of area-based R_h (g C m^{-2} $year^{-1}$) ($P < 0.001$, $R^2 = 0.89$; fig. S5), generating consistent patterns between CUE_{ST} and R_h under both R_h units (Fig. 3 and fig. S6). To minimize the errors caused by uncertainties in soil bulk density and sampling depth during unit conversions, we used the original unit of R_h (g C m^{-2} $year^{-1}$) instead of converting it to g C kg^{-1} $year^{-1}$ in subsequent analysis.

In addition, we collected 52 observations of average daily R_h from the 160 selected articles (fig. S7). This means that these studies included all parameters for estimating CUE_{ST} and measured average daily R_h simultaneously, thus ensuring an exact match between observations of average daily R_h and CUE_{ST} on both temporal and spatial scales.

Environmental variables

To identify the environmental drivers underlying the relationships between CUE_{ST} and R_h, we examined nine variables representing the four basic factors essential to microbial metabolism: temperature, water, C, and nutrients (*27*, *54*, *55*). Specifically, we used mean annual air temperature (MAT) and soil MAT for temperature; MAP for water; LAI, aboveground biomass (AGB), and belowground biomass (BGB) for C; and soil pH, CEC, and clay content as proxies for nutrient availability. In particular, we chose these nutrient-related variables instead of direct soil N and P indicators to avoid collinearity, as soil C, N, and P concentrations are already embedded in the stoichiometric model used to estimate CUE_{ST} (see the "Theoretical basis of the stoichiometric model" section). We retrieved MAT, soil MAT, MAP, LAI, AGB, BGB, CEC, and clay content from multiple sources at a relatively fine spatial resolution (see table S10 for details). In particular, soil pH observations were compiled primarily from the 160 screened studies, which almost always reported soil pH. Only 16 studies did not include soil pH, and we extracted these missing values ($n = 82$) from other recently published studies with the same sample site information and similar geographic coordinates.

Among the nine variables, we further chose four of them (soil temperature, MAP, LAI, and soil pH) as the key indicators representing temperature, water, C, and nutrients, respectively, to explore the specific effects of the four kinds of basic controls on CUE_{ST} and R_h. We choose soil MAT rather than MAT because soil temperatures are generally less variable than atmospheric temperatures (*56*). We used LAI as the key index of C availability for two reasons. First, almost all C sources in surface soil originally come from plant production, especially plant litter inputs. Second, plant litter rather than soil organic matter that has been processed by microorganisms is the dominant C source for microbial acquisition (*57*). Among three proxies of nutrient availability (soil pH, CEC, and clay content), soil pH is a basic regulator of the availabilities of N and P and indirectly represents their supplies (*58*, *59*). We thus adopted it as an indicator of the availabilities of soil N and P.

Estimating CUE_{ST} using the stoichiometric model

Theoretical basis of the stoichiometric model

Sinsabaugh and Follstad Shah (*24*) proposed a biogeochemical-equilibrium model that incorporated ecoenzymatic activities, microbial biomass, and soil resources to estimate CUE_{ST} at the community level. The basis of this stoichiometric approach is using selected ecoenzymatic activities to represent the requirements of microbial resources. Specifically, soil microorganisms synthesize and excrete a series of ecoenzymes (table S1) that degrade organic macromolecules into available substrates (e.g., oligo- and monomers) for microbial assimilation. The profile of ecoenzymatic activity therefore represents the relative microbial acquisition of C, N, and P resources from polymers that balance microbial stoichiometry, given the efficiencies of assimilating elements and resource availability (*24*). Many ecoenzymes contribute to the catabolism of complex polymers (e.g., cellulose), but only a few (i.e., BG, NAG and/or LAP, and AP) catalyze the terminal reactions of the most common substrates and produce soluble products for microbial assimilation. These ecoenzymes thus define the functional interface between product release and acquisition (*60*). They usually have the highest activities

per unit microbial biomass and are strongly associated with litter decay and microbial metabolism (*61*). As a result, they are commonly selected as the proximate agents for the acquisition of microbial nutrients during metabolism (*13*, *24*).

Estimating CUE$_{ST}$

In detail, we estimated CUE_{ST} using the following equations (*24*)

$$CUE_{ST} = CUE^{max} \times \left\{ \frac{(S_{C:N} \times S_{C:P})}{[(K_{C:N} + S_{C:N}) \times (K_{C:P} + S_{C:P})]} \right\}^{0.5} \quad (1)$$

$$S_{C:N} = \frac{B_{C:N}}{L_{C:N}} \times \frac{1}{EEA_{C:N}} \quad (2)$$

$$S_{C:P} = \frac{B_{C:P}}{L_{C:P}} \times \frac{1}{EEA_{C:P}} \quad (3)$$

where $S_{C:N}$ and $S_{C:P}$ are scalars that represent the extent to which the allocation of extracellular enzyme activity (EEA) offsets the disparity between the elemental composition of available resources and the composition of microbial biomass. In this case, $EEA_{C:N}$ and $EEA_{C:P}$ were calculated as BG/(NAG + LAP) and BG/AP, respectively. Furthermore, $L_{C:N}$ and $L_{C:P}$ were estimated as molar ratios of SOC:TN and SOC:TP, respectively, and $B_{C:N}$ and $B_{C:P}$ were calculated as molar ratios of MBC (microbial biomass C):MBN (microbial biomass N) and MBC:MBP (microbial biomass P), respectively. Both $K_{C:N}$ and $K_{C:P}$ are half-saturation constants for CUE_{ST} based on the availabilities of C, N, and P, assumed to be 0.5 (*24*). CUE^{max} (maximum CUE) is about 0.6 based on metabolic kinetics and energetics (*19*, *39*).

It is worth noting that the enzymatic activities we selected were generally proxies of microbial metabolism using polymeric organic matter (*24*, *61*). Soluble resources not requiring enzymatic catalysis for acquisition could potentially skew our estimates (*3*, *62*). We thus only retained observations of surface soils from natural ecosystems, where the original dominant nutrient pools should be polymer-rich organic matter from plant litter (*63*). This filtering could minimize uncertainties introduced by soluble resources such as rhizodeposition and fertilizers.

Dataset of $^{13}C/^{18}O$-based CUE for global natural ecosystems

For verifying the results relevant to CUE_{ST}, we also considered the results of CUE independently measured by the isotope-based approaches. We obtained a dataset of $^{13}C/^{18}O$-CUE at a global scale (fig. S7) from a recent study based on the meta-analysis (*6*). This study collected 132 observations of $^{13}C/^{18}O$-CUE measured at 46 locations from 16 publications. In cases of manipulation experiments (for example, fertilization experiments), only data from control plots was included. Therefore, the dataset only represents an investigation of CUE in natural ecosystems.

Statistical analyses

The locations of these sample sites for CUE_{ST}, R_h, and $^{13}C/^{18}O$-CUE were divided into four climatic zones (tropical, temperate, arid, and cold zones) on the basis of the global Köppen-Geiger grid map of climatic classification (*64*). We identified the relationships between CUE_{ST} (or $^{13}C/^{18}O$-CUE) and R_h (or average daily R_h) among climate zones and between low-productivity (LAI < 3) and high-productivity (LAI > 3) ecosystems using generalized linear models (Figs. 2 to 4). We also determined the patterns of decoupling between CUE_{ST} and R_h (or average daily R_h) at the global scale by first identifying their decoupling thresholds from a piecewise linear-regression analysis (Figs. 2C and 3C, fig. S6, and tables S4 to S6). The regression relationships between CUE_{ST} and R_h (or average daily R_h) were fitted with linear models using the "segmented" (version 2.1-3) R package (*65*). The confidence intervals of the thresholds were calculated using 1000 bootstrap samples and the "SiZer" (version 0.1-8) R package (*66*). In addition, we tested three nonlinear functions (exponential, logarithmic, and quadratic) for the relationships of CUE_{ST} versus R_h (fig. S4) and CUE_{ST} versus average daily R_h (fig. S8), fitted separately within low- and high-productivity ecosystems. These analyses corroborate the productivity-dependent relationships between CUE_{ST} and R_h: robust negative associations in low-productivity ecosystems and weak or near-zero relationships in high-productivity ecosystems.

To gauge bias from coordinate-based pairing, we ran a stratified random-removal sensitivity test using the "tidyverse" (version 2.0.0) and "broom" (version 1.0.7) R packages: We repeatedly removed 20% of CUE_{ST}-R_h pairs within climatic zones and separately within productivity classes and reidentified slopes of regressions between CUE_{ST} and R_h. The negative relationship persisted in arid and cold zones or in low-productivity ecosystems and remained weak or indistinguishable from zero in temperate and tropical zones or in high-productivity ecosystems (figs. S2 and S3 and tables S2 and S3), indicating that our conclusions are robust to plausible mismatching.

We further investigated the effects of resource availabilities on the relationships between CUE_{ST} and R_h for low- and high-productivity ecosystems. First, we examined the distribution of the newly defined variable (CUE_{ST}/R_h) with productivity groups by kernel density plots and formal normality tests. Both the plots and test results indicated that CUE_{ST}/R_h deviate from normality (Shapiro-Wilk, Lilliefors, and Anderson-Darling, all $P < 0.001$; fig. S9 and table S7). We therefore further verified robustness with (i) ordinary least squares on log-transformed CUE_{ST}/R_h with HC3 robust standard errors and (ii) gamma generalized linear models (log link) using the "lmtest" and "sandwich" (version 3.1-1) R packages (fig. S10 and tables S8 and S9). Second, an analysis of mixed-effects model selection was adopted to identify the most important predictors among the nine environmental variables affecting CUE_{ST}/R_h using the "glmulti" (version 1.0.8) R package (*67*). The model selection was based on maximum-likelihood estimation. The importance of each predictor was calculated as the sum of Akaike weights for models that included this predictor (Fig. 4, A and B, and fig. S12). A cutoff of 0.8 was set to differentiate between essential and nonessential predictors (*67*). The signs and relative importance patterns of nine environmental variables identified by robustness analysis were consistent with the results of mixed-effects models, which suggests that the analysis of mixed-effects model selection is reasonable and robust. Third, we separately identified the relationships between CUE_{ST}/R_h and nine environmental variables for low- and high-productivity ecosystems and for four climate zones using generalized linear models (Fig. 4C and fig. S12).

We also explored possible mechanisms affecting the relationships between CUE_{ST} and R_h by identifying the effects of the four key variables of the nine environmental variables on CUE_{ST} and R_h using multiple statistical analyses. First, a linear mixed-effects model was used to analyze the differences of the four variables among climatic zones (fig. S11). The model was constructed using the "lme"

function from the "nlme" (version 3.1-164) R package, with "climatic zone" as the fixed factor and "sampling site" as the random factor. Tukey's tests were further used to identify the significance of differences in variables among the climatic zones using the "multcompView" (version 0.1-10) R package. Second, the analysis of mixed-effects model selection was adopted to identify the most important predictors among the four key variables affecting CUE_{ST}/R_h, CUE_{ST}, and R_h separately (figs. S12 and S15). Third, the partial correlation analysis further identified specific relationships between each variable and CUE_{ST} (or R_h) by controlling the other three variables using the "pcor.test" function in the "ppcor" (version 1.1) R package (fig. S13). Fourth, we also used a variation-partitioning analysis to quantify the independent and joint influences of the four key variables on CUE_{ST} with R_h using the "varpart" function in the "vegan" (version 2.6-8) R package (fig. S12). We calculated the relative independent and joint influences of the four variables on CUE_{ST} and R_h to facilitate interpretation

$$\text{Independent relative influence} = \frac{\text{Independent explanation of each variable}}{\text{Total explanation of all variables}}$$

$$\text{Joint relative influence} = \frac{\text{Joint explanation of one with others}}{\text{Total explanation of all variables}}$$

All statistical analyses were performed using R software (version 4.4.2 for the original analyses and version 4.5.1 for the revision) (*68*).

Supplementary Materials

This PDF file includes:

Figs. S1 to S16
Tables S1 to S10
References

REFERENCES

1. Y. Kuzyakov, Sources of CO_2 efflux from soil and review of partitioning methods. *Soil Biol. Biochem.* **38**, 425–448 (2006).
2. B. Bond-Lamberty, V. L. Bailey, M. Chen, C. M. Gough, R. Vargas, Globally rising soil heterotrophic respiration over recent decades. *Nature* **560**, 80–83 (2018).
3. J. Schimel, M. N. Weintraub, D. L. Moorhead, Estimating microbial carbon use efficiency in soil: Isotope-based and enzyme-based methods measure fundamentally different aspects of microbial resource use. *Soil Biol. Biochem.* **169**, 108677 (2022).
4. S. Manzoni, P. Taylor, A. Richter, A. Porporato, G. I. Ågren, Environmental and stoichiometric controls on microbial carbon-use efficiency in soils. *New Phytol.* **196**, 79–91 (2012).
5. M. F. Cotrufo, J. L. Soong, A. J. Horton, E. E. Campbell, M. L. Haddix, D. H. Wall, W. J. Parton, Formation of soil organic matter via biochemical and physical pathways of litter mass loss. *Nat. Geosci.* **8**, 776–779 (2015).
6. F. Tao, Y. Huang, B. A. Hungate, S. Manzoni, S. D. Frey, M. W. Schmidt, M. Reichstein, N. Carvalhais, P. Ciais, L. Jiang, J. Lehmann, Y. Wang, B. Z. Houlton, B. Ahrens, U. Mishra, G. Hugelius, T. D. Hocking, X. Lu, Z. Shi, K. Viatkin, R. Vargas, Y. Yigini, C. Omuto, A. A. Malik, G. Peralta, R. Cuevas-Corona, L. E. Di Paolo, I. Luotto, C. Liao, Y. Liang, V. S. Saynes, X. Huang, Y. Luo, Microbial carbon use efficiency promotes global soil carbon storage. *Nature* **618**, 981–985 (2023).
7. S. B. Hagerty, K. J. Van Groenigen, S. D. Allison, B. A. Hungate, E. Schwartz, G. W. Koch, R. K. Kolka, P. Dijkstra, Accelerated microbial turnover but constant growth efficiency with warming in soil. *Nat. Clim. Change* **4**, 903–906 (2014).
8. T. P. Smith, T. Clegg, T. Bell, S. Pawar, Systematic variation in the temperature dependence of bacterial carbon use efficiency. *Ecol. Lett.* **24**, 2123–2133 (2021).
9. A. Nissan, U. Alcolombri, N. Peleg, N. Galili, J. Jimenez-Martinez, P. Molnar, M. Holzner, Global warming accelerates soil heterotrophic respiration. *Nat. Commun.* **14**, 3452 (2023).
10. C. Yue, J. Jian, P. Ciais, X. Ren, J. Jiao, S. An, Y. Li, J. Wu, P. Zhang, B. Bond-Lamberty, Field experiments show no consistent reductions in soil microbial carbon in response to warming. *Nat. Commun.* **15**, 1731 (2024).
11. J. Schroeder, C. Dămătîrcă, T. Bölscher, C. Chenu, L. Elsgaard, C. C. Tebbe, L. Skadell, C. Poeplau, Liming effects on microbial carbon use efficiency and its potential consequences for soil organic carbon stocks. *Soil Biol. Biochem.* **191**, 109342 (2024).
12. L. Fang, Multifaceted links between microbial carbon use efficiency and soil organic carbon sequestration. *Glob. Chang. Biol.* **31**, e70045 (2025).
13. R. G. Burns, R. P. Dick, *Enzymes in the Environment: Activity, Ecology, and Applications* (CRC Press, 2002).
14. C. Wang, Y. Kuzyakov, Energy use efficiency of soil microorganisms: Driven by carbon recycling and reduction. *Glob. Chang. Biol.* **29**, 6170–6187 (2023).
15. L. Qu, C. Wang, E. Bai, Evaluation of the ^{18}O-H_2O incubation method for measurement of soil microbial carbon use efficiency. *Soil Biol. Biochem.* **145**, 107802 (2020).
16. C. Wang, L. Qu, L. Yang, D. Liu, E. Morrissey, R. Miao, Z. Liu, Q. Wang, Y. Fang, E. Bai, Large-scale importance of microbial carbon use efficiency and necromass to soil organic carbon. *Glob. Change Biol.* **27**, 2039–2048 (2021).
17. J. Hu, C. Huang, S. Zhou, Y. Kuzyakov, Nitrogen addition to soil affects microbial carbon use efficiency: Meta-analysis of similarities and differences in ^{13}C and ^{18}O approaches. *Glob. Change Biol.* **28**, 4977–4988 (2022).
18. K. Yu, L. He, S. Niu, J. Wang, P. Garcia-Palacios, M. Dacal, C. Averill, K. Georgiou, J. Ye, F. Mo, L. Yang, T. W. Crowther, Nonlinear microbial thermal response and its implications for abrupt soil organic carbon responses to warming. *Nat. Commun.* **16**, 2763 (2025).
19. H. Doi, M. Cherif, T. Iwabuchi, I. Katano, J. C. Stegen, M. Striebel, Integrating elements and energy through the metabolic dependencies of gross growth efficiency and the threshold elemental ratio. *Oikos* **119**, 752–765 (2010).
20. J. E. Hobbie, E. A. Hobbie, Microorganisms in nature are limited by carbon and energy: The starving-survival lifestyle in soil and consequences for estimating microbial rates. *Front. Microbiol.* **4**, 324 (2013).
21. J. Chen, K. J. van Groenigen, B. A. Hungate, C. Terrer, J. W. van Groenigen, F. T. Maestre, S. C. Ying, Y. Luo, U. Jørgensen, R. L. Sinsabaugh, J. E. Olesen, L. Elsgaard, Long-term nitrogen loading alleviates phosphorus limitation in terrestrial ecosystems. *Glob. Change Biol.* **26**, 5077–5086 (2020).
22. Y. Cui, D. L. Moorhead, X. Wang, M. Xu, X. Wang, X. Wei, Z. Zhu, T. Ge, S. Peng, B. Zhu, L. Fang, Decreasing microbial phosphorus limitation increases soil carbon release. *Geoderma* **419**, 115868 (2022).
23. C. Averill, Divergence in plant and microbial allocation strategies explains continental patterns in microbial allocation and biogeochemical fluxes. *Ecol. Lett.* **17**, 1202–1210 (2014).
24. R. L. Sinsabaugh, J. J. Follstad Shah, Ecoenzymatic stoichiometry and ecological theory. *Annu. Rev. Ecol. Evol. Syst.* **43**, 313–343 (2012).
25. J. Jian, R. Vargas, K. Anderson-Teixeira, E. Stell, V. Herrmann, M. Horn, N. Kholod, J. Manzon, R. Marchesi, D. Paredes, B. Bond-Lamberty, A restructured and updated global soil respiration database (SRDB-V5). *Earth Syst. Sci. Data* **13**, 255–267 (2021).
26. L. Henneron, J. Balesdent, G. Alvarez, P. Barré, F. Baudin, I. Basile-Doelsch, L. Cécillon, A. Fernandez-Martinez, C. Hatté, S. Fontaine, Bioenergetic control of soil carbon dynamics across depth. *Nat. Commun.* **13**, 7676 (2022).
27. A. Hursh, A. Ballantyne, L. Cooper, M. Maneta, J. Kimball, J. Watts, The sensitivity of soil respiration to soil temperature, moisture, and carbon supply at the global scale. *Glob. Change Biol.* **23**, 2090–2103 (2017).
28. E. Du, C. Terrer, A. F. Pellegrini, A. Ahlström, C. J. van Lissa, X. Zhao, N. Xia, X. Wu, R. B. Jackson, Global patterns of terrestrial nitrogen and phosphorus limitation. *Nat. Geosci.* **13**, 221–226 (2020).
29. Y. Cui, H. Bing, D. L. Moorhead, M. Delgado-Baquerizo, L. Ye, J. Yu, S. Zhang, X. Wang, S. Peng, X. Guo, B. Zhu, J. Chen, W. Tan, Y. Wang, X. Zhang, L. Fang, Ecoenzymatic stoichiometry reveals widespread soil phosphorus limitation to microbial metabolism across Chinese forests. *Commun. Earth Environ.* **3**, 1–8 (2022).
30. Y. Cui, S. Peng, M. C. Rillig, T. Camenzind, M. Delgado-Baquerizo, C. Terrer, X. Xu, M. Feng, M. Wang, L. Fang, B. Zhu, E. Du, D. L. Moorhead, R. L. Sinsabaugh, J. Peñuelas, J. J. Elser, Global patterns of nutrient limitation in soil microorganisms. *Proc. Natl. Acad. Sci. U.S.A.* **122**, e2424552122 (2025).
31. A. T. Nottingham, B. L. Turner, A. W. Stott, E. V. Tanner, Nitrogen and phosphorus constrain labile and stable carbon turnover in lowland tropical forest soils. *Soil Biol. Biochem.* **80**, 26–33 (2015).
32. J. Helfenstein, F. Tamburini, C. von Sperber, M. S. Massey, C. Pistocchi, O. A. Chadwick, P. M. Vitousek, R. Kretzschmar, E. Frossard, Combining spectroscopic and isotopic techniques gives a dynamic view of phosphorus cycling in soil. *Nat. Commun.* **9**, 3226 (2018).
33. M. F. Cotrufo, M. D. Wallenstein, C. M. Boot, K. Denef, E. Paul, The Microbial Efficiency-Matrix Stabilization (MEMS) framework integrates plant litter decomposition with soil organic matter stabilization: do labile plant inputs form stable soil organic matter? *Glob. Change Biol.* **19**, 988–995 (2013).
34. E. M. Morrissey, R. L. Mau, E. Schwartz, T. A. McHugh, P. Dijkstra, B. J. Koch, J. C. Marks, B. A. Hungate, Bacterial carbon use plasticity, phylogenetic diversity and the priming of soil organic matter. *ISME J.* **11**, 1890–1899 (2017).

35. M. A. Bradford, R. L. McCulley, T. W. Crowther, E. E. Oldfield, S. A. Wood, N. Fierer, Cross-biome patterns in soil microbial respiration predictable from evolutionary theory on thermal adaptation. *Nat. Ecol. Evol.* **3**, 223–231 (2019).
36. J. Lehmann, M. Kleber, The contentious nature of soil organic matter. *Nature* **528**, 60–68 (2015).
37. T. Camenzind, S. Hättenschwiler, K. K. Treseder, A. Lehmann, M. C. Rillig, Nutrient limitation of soil microbial processes in tropical forests. *Ecol. Monogr.* **88**, 4–21 (2018).
38. X. Fan, E. Bai, J. Zhang, X. Wang, W. Yuan, S. Piao, The carbon transfer from plant to soil is more efficient in less productive ecosystems. *Global Biogeochem. Cy.* **37**, e2023GB007727 (2023).
39. A. P. Allen, J. F. Gillooly, Towards an integration of ecological stoichiometry and the metabolic theory of ecology to better understand nutrient cycling. *Ecol. Lett.* **12**, 369–384 (2009).
40. S. Manzoni, A. Porporato, Soil carbon and nitrogen mineralization: Theory and models across scales. *Soil Biol. Biochem.* **41**, 1355–1379 (2009).
41. Z. Zhu, S. Piao, R. B. Myneni, M. Huang, Z. Zeng, J. G. Canadell, P. Ciais, S. Sitch, P. Friedlingstein, A. Arneth, C. Cao, L. Cheng, E. Kato, C. Koven, Y. Li, X. Lian, Y. Liu, R. Liu, J. Mao, Y. Pan, S. Peng, J. Peñuelas, B. Poulter, T. A. M. Pugh, B. D. Stocker, N. Viovy, X. Wang, Y. Wang, Z. Xiao, H. Yang, S. Zaehle, N. Zeng, Greening of the Earth and its drivers. *Nat. Clim. Change* **6**, 791–795 (2016).
42. IPCC, *Climate Change 2022: Impacts, Adaptation and Vulnerability. IPCC Sixth Assessment Report* (IPCC, 2022).
43. Y. Wang, J. Xiao, Y. Ma, J. Ding, X. Chen, Z. Ding, Y. Luo, Persistent and enhanced carbon sequestration capacity of alpine grasslands on Earth's Third Pole. *Sci. Adv.* **9**, eade6875 (2023).
44. S. Piao, Q. Liu, A. Chen, I. A. Janssens, Y. Fu, J. Dai, L. Liu, X. Lian, M. Shen, X. Zhu, Plant phenology and global climate change: Current progresses and challenges. *Glob. Change Biol.* **25**, 1922–1940 (2019).
45. J. Tian, J. A. Dungait, X. Lu, Y. Yang, I. P. Hartley, W. Zhang, J. Mo, G. Yu, J. Zhou, Y. Kuzyakov, Long-term nitrogen addition modifies microbial composition and functions for slow carbon cycling and increased sequestration in tropical forest soil. *Glob. Chang. Biol.* **25**, 3267–3281 (2019).
46. Z. Mou, L. Kuang, J. Zhang, Y. Li, W. Wu, C. Liang, D. Hui, H. Lambers, J. Sardans, J. Peñuelas, J. Liu, H. Ren, Z. Liu, Nutrient availability and stoichiometry mediate microbial effects on soil carbon sequestration in tropical forests. *Soil Biol. Biochem.* **186**, 109186 (2023).
47. J. Penuelas, B. Poulter, J. Sardans, P. Ciais, M. Van Der Velde, L. Bopp, O. Boucher, Y. Godderis, P. Hinsinger, J. Llusia, E. Nardin, S. Vicca, M. Obersteiner, I. A. Janssens, Human-induced nitrogen-phosphorus imbalances alter natural and managed ecosystems across the globe. *Nat. Commun.* **4**, 2934 (2013).
48. G. Yu, Y. Jia, N. He, J. Zhu, Z. Chen, Q. Wang, S. Piao, X. Liu, H. He, X. Guo, Z. Wen, P. Li, G. Ding, K. Goulding, Stabilization of atmospheric nitrogen deposition in China over the past decade. *Nat. Geosci.* **12**, 424–429 (2019).
49. D. L. Jones, E. C. Cooledge, F. C. Hoyle, R. I. Griffiths, D. V. Murphy, pH and exchangeable aluminum are major regulators of microbial energy flow and carbon use efficiency in soil microbial communities. *Soil Biol. Biochem.* **138**, 107584 (2019).
50. C. L. Lauber, M. Hamady, R. Knight, N. Fierer, Pyrosequencing-based assessment of soil pH as a predictor of soil bacterial community structure at the continental scale. *Appl. Environ. Microbio.* **75**, 5111–5120 (2009).
51. P. Čapek, S. Manzoni, E. Kaštovská, B. Wild, K. Diáková, J. Bárta, J. Schnecker, C. Biasi, P. J. Martikainen, R. J. Eloy Alves, G. Guggenberger, N. Gentsch, G. Hugelius, J. Palmtag, R. Mikutta, O. Shibistova, T. Urich, C. Schleper, A. Richter, H. Šantrůčková, A plant-microbe interaction framework explaining nutrient effects on primary production. *Nat. Ecol. Evol.* **2**, 1588–1596 (2018).
52. J. L. DeForest, D. L. Moorhead, Effects of elevated pH and phosphorus fertilizer on soil C, N and P enzyme stoichiometry in an acidic mixed mesophytic deciduous forest. *Soil Biol. Biochem.* **150**, 107996 (2020).
53. Y. Cui, J. Hu, S. Peng, M. Delgado-Baquerizo, D. L. Moorhead, R. L. Sinsabaugh, X. Xu, K. M. Geyer, L. Fang, P. Smith, J. Peñuelas, Y. Kuzyakov, J. Chen, Limiting resources define the global pattern of soil microbial carbon use efficiency. *Adv. Sci.* **11**, e2308176 (2024).
54. T. W. Crowther, J. Van den Hoogen, J. Wan, M. A. Mayes, A. D. Keiser, L. Mo, C. Averill, D. S. Maynard, The global soil community and its influence on biogeochemistry. *Science* **365**, eaav0550 (2019).
55. L. Philippot, C. Chenu, A. Kappler, M. C. Rillig, N. Fierer, The interplay between microbial communities and soil properties. *Nat. Rev. Microbiol.* **22**, 226–239 (2024).
56. J. J. Lembrechts, J. van den Hoogen, J. Aalto, M. B. Ashcroft, P. De Frenne, J. Kemppinen, M. Kopecký, M. Luoto, I. M. D. Maclean, T. W. Crowther, J. J. Bailey, S. Haesen, D. H. Klinges, P. Niittynen, B. R. Scheffers, K. Van Meerbeek, P. Aartsma, O. Abdalaze, M. Abedi, R. Aerts, N. Ahmadian, A. Ahrends, J. M. Alatalo, J. M. Alexander, C. N. Allonsius, J. Altman, C. Ammann, C. Andres, C. Andrews, J. Ardö, N. Arriga, A. Arzac, V. Aschero, R. L. Assis, J. J. Assmann, M. Y. Bader, K. Bahalkeh, P. Barančok, I. C. Barrio, A. Barros, M. Barthel, E. W. Basham, M. Bauters, M. Bazzichetto, L. B. Marchesini, M. C. Bell, J. C. Benavides, J. L. B. Alonso, B. J. Berauer, J. W. Bjerke, R. G. Björk, M. P. Björkman, K. Björnsdóttir, B. Blonder, P. Boeckx, J. Boike, S. Bokhorst, B. N. S. Brum, J. Brůna, N. Buchmann, P. Buysse, J. L. Camargo, O. C. Campoe, O. Candan, R. Canessa, N. Cannone, M. Carbognani, J. Carnicer, A. Casanova-Katny, S. Cesarz, B. Chojnicki, P. Choler, S. L. Chown, E. F. Cifuentes, M. Čiliak, T. Contador, P. Convey, E. J. Cooper, E. Cremonese, S. R. Curasi, R. Curtis, M. Cutini, C. J. Dahlberg, G. N. Daskalova, M. A. de Pablo, S. D. Chiesa, J. Dengler, B. Deronde, P. Descombes, V. D. Cecco, M. D. Musciano, J. Dick, R. D. Dimarco, J. Dolezal, E. Dorrepaal, J. Dušek, N. Eisenhauer, L. Eklundh, T. E. Erickson, B. Erschbamer, W. Eugster, R. M. Ewers, D. A. Exton, N. Fanin, F. Fazlioglu, I. Feigenwinter, G. Fenu, O. Ferlian, M. R. F. Calzado, E. Fernández-Pascual, M. Finckh, R. F. Higgens, T. G. W. Forte, E. C. Freeman, E. R. Frei, E. Fuentes-Lillo, R. A. García, M. B. García, C. Géron, M. Gharun, D. Ghosn, K. Gigauri, A. Gobin, I. Goded, M. Goeckede, F. Gottschall, K. Goulding, S. Govaert, B. J. Graae, S. Greenwood, C. Greiser, A. Grelle, B. Guénard, M. Guglielmin, J. Guillemot, P. Haase, S. Haider, A. H. Halbritter, M. Hamid, A. Hammerle, A. Hampe, S. V. Haugum, L. Hederová, B. Heinesch, C. Helfter, D. Hepenstrick, M. Herberich, M. Herbst, L. Hermanutz, D. S. Hik, R. Hoffrén, J. Homeier, L. Hörtnagl, T. T. Høye, F. Hrbacek, K. Hylander, H. Iwata, M. A. Jackowicz-Korczynski, H. Jactel, J. Järveoja, S. Jastrzębowski, A. Jentsch, J. J. Jiménez, I. S. Jónsdóttir, T. Jucker, A. S. Jump, R. Juszczak, R. Kanka, V. Kašpar, G. Kazakis, J. Kelly, A. A. Khuroo, L. Klemedtsson, M. Klisz, N. Kljun, A. Knohl, J. Kobler, J. Kollár, M. M. Kotowska, B. Kovács, J. Kreyling, A. Lamprecht, S. I. Lang, C. Larson, K. Larson, K. Laska, G. le Maire, R. I. Leihy, L. Lens, B. Liljebladh, A. Lohila, J. Lorite, B. Loubet, J. Lynn, M. Macek, R. Mackenzie, E. Magliulo, R. Maier, F. Malfasi, F. Máliš, M. Man, G. Manca, A. Manco, T. Manise, P. Manolaki, F. Marciniak, R. Matula, A. C. Mazzolari, S. Medinets, V. Medinets, C. Meeussen, S. Merinero, R. de Cássia Guimarães Mesquita, K. Meusburger, F. J. R. Meysman, S. T. Michaletz, A. Milbau, D. Moiseev, P. Moiseev, A. Mondoni, R. Monfries, L. Montagnani, M. Moriana-Armendariz, U. M. di Cella, M. Mörsdorf, J. R. Mosedale, L. Muffler, M. Muñoz-Rojas, J. A. Myers, I. H. Myers-Smith, L. Nagy, M. Nardino, I. Naujokaitis-Lewis, E. Newling, L. Nicklas, G. Niedrist, A. Niessner, M. B. Nilsson, S. Normand, M. D. Nosetto, Y. Nouvellon, M. A. Nuñez, R. Ogaya, J. Ogée, J. Okello, J. Olejnik, J. E. Olesen, Ø. H. Opedal, S. Orsenigo, A. Palaj, T. Pampuch, A. V. Panov, M. Pärtel, A. Pastor, A. Pauchard, H. Pauli, M. Pavelka, W. D. Pearse, M. Peichl, L. Pellissier, R. M. Penczykowski, J. Penuelas, M. P. Bon, A. Petraglia, S. S. Phartyal, G. K. Phoenix, C. Pio, A. Pitacco, C. Pitteloud, R. Plichta, F. Porro, M. Portillo-Estrada, J. Poulenard, R. Poyatos, A. S. Prokushkin, R. Puchalka, M. Puşcaş, D. Radujković, K. Randall, A. R. Backes, S. Remmele, W. Remmers, D. Renault, A. C. Risch, C. Rixen, S. A. Robinson, B. J. M. Robroek, A. V. Rocha, C. Rossi, G. Rossi, O. Roupsard, A. V. Rubtsov, P. Saccone, C. Sagot, J. S. Bravo, C. C. Santos, J. M. Sarneel, T. Scharnweber, J. Schmeddes, M. Schmidt, T. Scholten, M. Schuchardt, N. Schwartz, T. Scott, J. Seeber, A. C. S. de Andrade, T. Seipel, P. Semenchuk, R. A. Senior, J. M. Serra-Diaz, P. Sewerniak, A. Shekhar, N. V. Sidenko, L. Siebicke, L. S. Collier, E. Simpson, D. P. Siqueira, Z. Sitková, J. Six, M. Smiljanic, S. W. Smith, S. Smith-Tripp, B. Somers, M. V. Sørensen, J. J. L. L. Souza, B. I. Souza, A. S. Dias, M. J. Spasojevic, J. D. M. Speed, F. Spicher, A. Stanisci, K. Steinbauer, R. Steinbrecher, M. Steinwandter, M. Stemkovski, J. G. Stephan, C. Stiegler, S. Stoll, M. Svátek, M. Svoboda, T. Tagesson, A. J. Tanentzap, F. Tanneberger, J.-P. Theurillat, H. J. D. Thomas, A. D. Thomas, K. Tielbörger, M. Tomaselli, U. A. Treier, M. Trouillier, P. D. Turtureanu, R. Tutton, V. A. Tyystjärvi, M. Ueyama, K. Ujházy, M. Ujházyová, D. Uogintas, A. V. Urban, J. Urban, M. Urbaniak, T.-M. Ursu, F. P. Vaccari, S. Van de Vondel, L. van den Brink, M. Van Geel, V. Vandvik, P. Vangansbeke, A. Varlagin, G. F. Veen, E. Veenendaal, S. E. Venn, H. Verbeeck, E. Verbrugggen, F. G. A. Verheijen, L. Villar, L. Vitale, P. Vittoz, M. Vives-Ingla, J. von Oppen, J. Walz, R. Wang, Y. Wang, R. G. Way, R. E. M. Wedegärtner, R. Weigel, J. Wild, M. Wilkinson, M. Wilmking, L. Wingate, M. Winkler, S. Wipf, G. Wohlfahrt, G. Xenakis, Y. Yang, Z. Yu, K. Yu, F. Zellweger, J. Zhang, Z. Zhang, P. Zhao, K. Zieblińska, R. Zimmermann, S. Zong, V. I. Zyryanov, I. Nijs, J. Lenoir, Global maps of soil temperature. *Glob. Change Biol.* **28**, 3110–3144 (2022).
57. Y. Cui, S. Peng, M. Delgado-Baquerizo, M. C. Rillig, C. Terrer, B. Zhu, X. Jing, J. Chen, J. Li, J. Feng, Y. He, L. Fang, D. L. Moorhead, R. L. Sinsabaugh, J. Peñuelas, Microbial communities in terrestrial surface soils are not widely limited by carbon. *Glob. Chang. Biol.* **29**, 4412–4429 (2023).
58. D. Curtin, C. A. Campbell, A. Jalil, Effects of acidity on mineralization: pH-dependence of organic matter mineralization in weakly acidic soils. *Soil Biol. Biochem.* **30**, 57–64 (1998).
59. N. J. Barrow, Comparing two theories about the nature of soil phosphate. *Eur. J. Soil Syst.* **72**, 679–685 (2021).
60. R. L. Sinsabaugh, B. H. Hill, J. J. Follstad Shah, Ecoenzymatic stoichiometry of microbial organic nutrient acquisition in soil and sediment. *Nature* **462**, 795–798 (2009).
61. D. L. Moorhead, R. L. Sinsabaugh, A theoretical model of litter decay and microbial interaction. *Ecol. Monogr.* **76**, 151–174 (2006).
62. D. L. Moorhead, Y. Cui, R. L. Sinsabaugh, J. Schimel, Interpreting patterns of ecoenzymatic stoichiometry. *Soil Biol. Biochem.* **180**, 108997 (2023).
63. M. F. Cotrufo, J. M. Lavallee, Soil organic matter formation, persistence, and functioning: A synthesis of current understanding to inform its conservation and regeneration. *Adv. Agron.* **172**, 1–66 (2022).
64. H. E. Beck, N. E. Zimmermann, T. R. McVicar, N. Vergopolan, A. Berg, E. F. Wood, Present and future Köppen-Geiger climate classification maps at 1-km resolution. *Sci. Data* **5**, 1–12 (2018).

65. V. M. R. Muggeo, Segmented: An R package to fit regression models with broken-line relationships. *R News* **8**, 20–25 (2008).
66. J. D. Toms, M. Lesperance, Piecewise regression: A tool for identifying ecological thresholds. *Ecology* **84**, 2034–2041 (2003).
67. V. Calcagno, C. de Mazancourt, glmulti: An R package for easy automated model selection with (generalized) linear models. *J. Stat. Softw.* **34**, 1–29 (2010).
68. R Core Team, "R: A language and environment for statistical computing" (R Foundation for Statistical Computing, 2024); www.R-project.org/.
69. R. L. Sinsabaugh, B. L. Turner, J. M. Talbot, B. G. Waring, J. S. Powers, C. R. Kuske, D. L. Moorhead, J. J. Follstad Shah, Stoichiometry of microbial carbon use efficiency in soils. *Ecol. Monogr.* **86**, 172–189 (2016).
70. S. Manzoni, Flexible carbon-use efficiency across litter types and during decomposition partly compensates nutrient imbalances-results from analytical stoichiometric models. *Front. Microbiol.* **8**, 661 (2017).
71. S. Manzoni, P. Čapek, M. Mooshammer, B. D. Lindahl, A. Richter, H. Šantrůčková, Optimal metabolic regulation along resource stoichiometry gradients. *Ecol. Lett.* **20**, 1182–1191 (2017).
72. A. Gunina, Y. Kuzyakov, From energy to (soil organic) matter. *Glob. Change Biol.* **28**, 2169–2182 (2022).
73. S. E. Fick, R. J. Hijmans, WorldClim 2: New 1km spatial resolution climate surfaces for global land areas. *Int. J. Climatol.* **37**, 4302–4315 (2017).
74. J. Mao, B. Yan, "Global monthly mean leaf area index climatology, 1981–2015" (ORNL Distributed Active Archive Center (DAAC), Oak Ridge National Laboratory, 2019); https://doi.org/10.3334/ORNLDAAC/1653.
75. S. A. Spawn, H. K. Gibbs, "Global aboveground and belowground biomass carbon density maps for the year 2010" (ORNL Distributed Active Archive Center (DAAC), Oak Ridge National Laboratory, 2020); https://doi.org/10.3334/ORNLDAAC/1763.
76. W. Shangguan, Y. Dai, Q. Duan, B. Liu, H. Yuan, A global soil data set for earth system modeling. *J. Adv. Model. Earth Syst.* **6**, 249–263 (2014).

Acknowledgments: We thank all the scientists who shared the original data for this study. We are also grateful to the reviewers for constructive comments and valuable suggestions that helped improve our manuscript. We appreciate P. Čapek for helpful suggestions on an earlier version of the manuscript. **Funding:** Y.C. acknowledges support from the National Natural Science Foundation of China (32101378) and Research Fellowship of the Alexander von Humboldt Foundation. J.P. acknowledges support from the Spanish Government grant PID2022-140808NB-I00, funded by MCIN, AEI/10.13039/ 501100011033 European Union Next Generation EU/PRTR, and the European Union grant CONCERTO (HORIZON-CL5-2024-D1-01). J.C. acknowledges support from the Aarhus Universitets Forskningsfond (AUFF-E-2019-7-1) and Danish Independent Research Foundation (1127-00015B). The publication of this study is financially supported by Open Access funds of Freie Universität Berlin. **Author contributions:** Conceptualization: Y.C., S.P., D.L.M., R.L.S., J.P., M.D.-B., Y.K., and M.C.R. Resources: Y.C., J.P., J.C., and M.C.R. Investigation: Y.C., J.P., C.T., and M.D.-B. Data curation: Y.C. Methodology: Y.C., S.P., D.L.M., R.L.S., J.P., and C.T. Software: Y.C. Formal analysis: Y.C., J.P., and J.C. Validation: Y.C., J.P., Y.K., and J.C. Visualization: Y.C., Y.K., and J.P. Funding acquisition: Y.C., J.P., J.C., and M.C.R. Project administration: Y.C., J.P., and J.C. Writing—original draft: Y.C., M.D.-B., R.L.S., and M.C.R. Writing—review and editing: Y.C., S.P., M.D.-B., D.L.M., R.L.S., C.T., T.P.S., Y.K., J.P., B.Z., F.T., S.B., J.C., and M.C.R. Supervision: Y.C., R.L.S., Y.K., J.P., J.C., and M.C.R. **Competing interests:** The authors declare that they have no competing interests. **Data and materials availability:** All data and code needed to evaluate and reproduce the results in the paper are present in the paper and/or the Supplementary Materials. All data used in this study are available in the Supplementary Materials or at Dryad (https://doi.org/10.5061/dryad.8cz8w9h49). The code used in this study is available at Figshare (https://doi.org/10.6084/m9.figshare.30350593).

Submitted 4 June 2025
Accepted 15 December 2025
Published 14 January 2026
10.1126/sciadv.adz5319